Correlation between austempering parameters and hardness of austempered ductile iron based on artificial neural network

Xuhong Guo*

School of Mechanical and Electric Engineering, Soochow University, Suzhou- Jiangsu, China

Abstract

Mechanical properties of ADI mainly depend on the austempering parameters, which include austenitizing temperature and time, austempering time and temperature, apart from chemical composition, alloyed elements and casting parameters. In this paper, an investigation has been conducted on the prediction model of mechanical properties of ADI between austenitizing temperature and time, austempering temperature and time as inputs and Vickers hardness of samples after austempering as the outputs based on artificial neural network. There are two types of data of the model: training data and testing data. The former data come from the published literature and 12 experimental data used for network testing. The research results of the model shows that the predicted values approach to the measured data in most of the testing samples and the maximum margin of error between experimental and predicted data is 4.682%.

Keywords: Austempered Ductile Iron, Artificial Neural Network, Austempering Parameters, Mechanical Properties, Prediction Model

1 Introduction

In recent years, austempered ductile iron (ADI) has been attracted much attention due to its exceptional combination of strength, hardness, impact resistance and ductility [1, 2, 3]. The attractive properties are related to its unique microstructure known as ausferrite, which is a mixture of bainitic ferrite (α) and high carbon austenite (γ_{HC}) [4, 5, 6]. Hence, ADI has been applied in many areas, such as automobile, aerospace, agricultural machinery, railroads and so on. S.F. LIU et al [7] indicated that the Mn-Cu alloyed ADI standard sample could reach European standard EN1564-97/EN-Cl5-1000-5 and could replace 20CrMnTi forged steel for manufacturing the EQ140 helical bevel gears. J.F. Dias [8] investigated reducing the austempering time increased the fatigue life and did not affect the mechanical properties or the rate of fatigue crack propagation, and could used for mechanical parts with stress riser details.

Mechanical properties of ADI mainly depend on the austempering parameters, which include austenitizing temperature and time, austempering time and temperature, apart from chemical composition, alloyed elements and casting parameters. It has been investigated [9] that the morphology of bainite and the fraction of retained austenite depend largely on the austempering temperature, which is one of the most important factors to affect the mechanical properties of ADI. The microstructure of ADI is mixture of finer ferrite and retained austenite when austempered at lower temperatures (230~350℃) and these results in higher tensile strength and hardness but with lower ductility. On the other hand, it is compound of coarser or feathery ferrite and austenite when austempered at higher temperatures (350~400℃) and this leads to lower tensile strength and hardness but with higher ductility.

It is known that the toughness of a material decreases as its strength increases. To improve the toughness of ADI meanwhile without reducing the strength, researchers presented a new and improved isothermal heat treatment to meet this demand. Susil K. Putatunda [10, 11] proposed a novel and innovative concept of two-step austempering process, which was used to produce ADI with simultaneous high yield strength and fracture toughness. Generally, two-step austempering process acquired higher combination of hardness and ductility compare with the single-step. This is mainly due to that, the former process obtained finer microstructure than the latter [12].

Alloyed elements such as nickel, copper and boron are usually added to strengthen the mechanical properties of ADI. Alloying of ADI with Ni and Mo increased its fracture toughness but decreased its tensile strength and hardness in the heat treated condition [13]. The Cu-alloyed ADI has better impact toughness and fracture toughness than does the unalloyed one because of copper increases the retained austenite content in ADI [14]. With higher boron content, the mechanical properties of CADI such as hardenability and toughness are found to decreases [15].

A significant number of studies have been carried out on the mechanical properties of ADI, but few studies have examined the correlation between the mechanical properties of ADI and influencing factors, such as

---

Corresponding author e-mail: huangxing8677@163.com

austempering parameters, the percentage of chemical composition and alloyed element and so on. M.A.Yescas [16] has been estimated of the fraction of retained austenite in ADI as a function of their chemical composition (C, Mn, Si, Ni, Mo, Cu) and the austempering parameters. H.PourAsiabi [17] has been developed a multi-layer perceptron artificial neural network model, which used Mo%, Cu%, austempering time and temperature as inputs and the Vickers hardness of samples after austempering as the output. However, very little is currently available in literature on the mechanical properties of unalloyed ADI with low manganese content.

However, very little information is currently available in literature on the mechanical properties of unalloyed ADI with austempering parameters. Specifically, the non-linear correlation of austenitizing temperature and time, austempering temperature and time as the inputs variable and the hardness of unalloyed ADI as the output are not clearly established. The main purpose of this work is to investigate the mechanical property prediction model between austenitizing temperature and time, austempering temperature and time as inputs and Vickers hardness of samples after austempering as the output based on artificial neural network.

2 Experimental details

The chemical composition of as-cast ductile iron in weight percent is reported in Table 1. The microstructure of as-cast ductile iron, which used in austempering experiment is shown in Fig. 1. The rate of graphite spheroidization is above 90% (level 3) and the diameter of the graphite nodule reach level-6. As-cast ductile iron is a mixture of pearlite, ferrite (about 40%) and graphite nodule.

TABLE 1 Chemical composition of as-cast ductile iron (*wt*%)

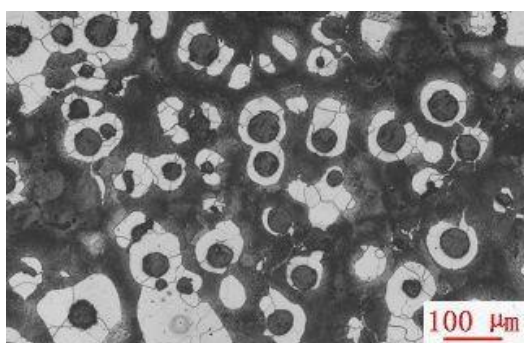| C	Si	Mn	P	S	Mg	Re	Al	Ti
3.65	2.78	0.32	0.026	0.009	0.042	0.025	0.015	0.002

FIGURE 1 Microstructures of as-cast ductile iron

Austempering process was conducted by first austenitizing the as-cast ductile iron by heating to 900℃ in an induction furnace and holding the temperature at that level for 2h. Then quickly quenched in a salt bath down to the austempering temperature at 400℃, 350℃,

300℃ and 250℃, in which a holding time was chosen as 1h, 2h and 3h, respectively, for each austempering temperature. Finally, the samples were immediately cooled in air to room temperature. 12 samples with different heat treating cycles were obtained and the detailed austempering parameters used for this study is shown in Fig. 2.
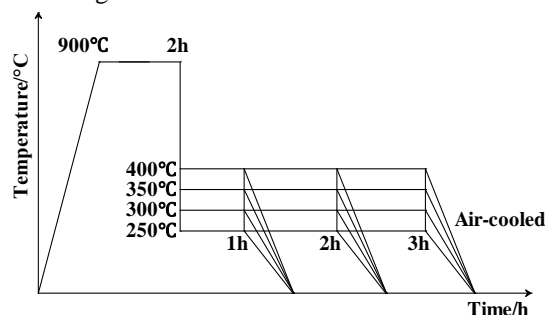

FIGURE 2 Austempering parameters schematic

The hardness of the samples after the austempering process was evaluated using by HB-3000 Brinell hardness tester, under 3000 kgf loading according to GB/T 231.1-2009. Three times were taken for each specimen and then the results were averaged.

3 Artificial neural network

Artificial neural network (ANN) is a mathematical model that can learn and generalize the things learned, especially suitable for non-linear properties from input to output [18]. Therefore, there is growing interest for development of intelligent dynamic systems based on practical data. Back propagation (BP), which is one of the most famous training algorithms for multilayer perceptions, is a gradient descent technique to minimise the error for particular training pattern [19].

The neuron is the basic part of artificial neural network. In general, each input is multiplied by its related weight and add together, plus the threshold value and then cross through activation functions to produce the outputs [20]. Fig. 3 shows the data processing in a neural network cell and the output of the neuron as Eq.1.
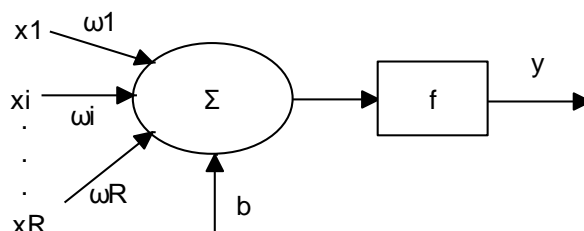

FIGURE 3 The data processing in a neural network cell

$$y = f(\sum_{i=1}^{R} x_i w_i + b),\qquad(1)$$

where x_i is normalized input variable, w_i is the weight of that variable, b is the threshold value, R is the number of the input variables, f is the activation

function of the cell and y is the network output of the cell.

Generally, the activation function is one of the most parts in neural network modeling, and the function is continues and derivative. Mean Square Error (MSE) as statistical criterion are utilized to evaluate results accuracy according to following equation:

$$MSE = \frac{1}{n}\sum_{j=1}^{n}(t_j - o_j)^2 , \qquad (2)$$

where t_j and o_j is target and predicted values respectively, n is the number of the network outputs [21, 22].

A typical BP-ANN model include three layers: input layer, one hidden layer and output layer. Full connection occurs among neurons belonging to each layer, while no connections exist among neurons belonging to the same layer. The weight of each layers can be adjust through network training. Generally, there are two types of data of the model: training data and testing data. 121 groups of data [1, 8, 9, 11, 12, 23, 24, 25, 26, 27, 28, 29, 30, 31, 32], which come from the published document, are designed for model training in this research. 12 experimental data used for network testing. To remove the order of magnitude from different input and output parameters, the data are disposed by using normalized method, which is set data between [0 1] (Eq. 3). After network testing is done, the outputs were reverse normalized (Eq. 4).

$$x_k = \frac{x_k - x_{min}}{x_{max} - x_{min}} , \qquad (3)$$

$$x_k = x_{min} + (x_{max} - x_{min})x_k , \qquad (4)$$

where x_{min} is the minimum value of each column, x_{max} is the maximum value of each column.

The schematic structure of this designed neural network is shown in Fig. 4. A BP-ANN model was used with austenitizing temperature and time, austempering temperature and time as inputs and the Rockwell hardness of ADI as the output of the model. The number of hidden layer selected 11 neurons on the basis of the previous empiric formulas. The activation function of the hidden layer uses a hyperbolic tangent sigmoid (tansig), while the output layer uses a linear (purelin) transfer function.
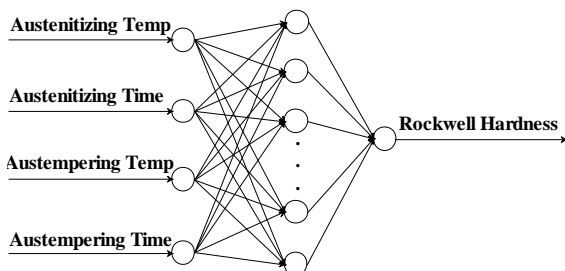

FIGURE 4 The schematic structure of this designed neural network

4 Results and discussion

The variation of hardness as a function of austempering temperature for austempering time 60, 120 and 180 min is shown in Fig. 5. It can be found that increase austempering temperature leads to a linear decrease in hardness at all times. It is mainly due to that the microstructure of ADI is mixture of finer ferrite and retained austenite when austempered under 350 ℃, and this results in higher tensile strength and hardness but lower ductility. On the other hand, it has a compound of coarser ferrite and austenite when austempered over 350 ℃, and this reduces to the yield and hardness strengths but with higher ductility.
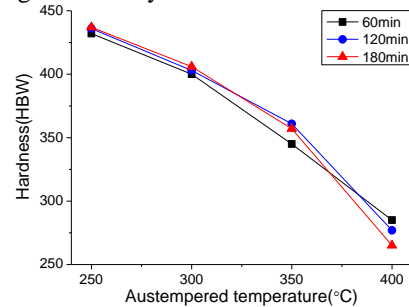

FIGURE 5 Influence of austempering temperatures on hardness at different austempering time

It is clearly observed that the hardness of ADI slightly change at different austempering time under the same temperature. Untransformed supercooling austenite, which under compressive stress gradually lose change activity and then transform into retained austenite when the austempering time more than 60 minute. On the other hand, the rate of bainite transformation increasingly slow and basically finished as the time over 60 minute [33]. It is apparently state that the austempering temperature has greatly impact on the hardness of ADI and the time has little or no effect on it.

The mean square error (MSE) value during network training is shown in Fig.6. It is evidenced that the training step have significant effect on the error of the network, in which MSE firstly decreases with the training step ranging from 0 to 300 epochs, and then it keep constant with further increasing training step. It is obviously found, that the order of magnitudes of the error approached to 10^{-3}, which indicates the desired network error achieved after training.
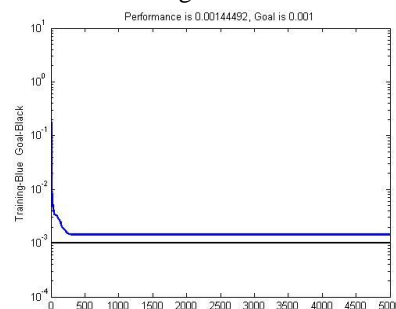

FIGURE 6 The variation of mean squared error (MSE) with number of epochs

74

The detailed mathematical equation of the neural network model is available after the network training and the formula of the model is as follows (Eq. 5):

$$T = f_2[w_2 f_1(w_1 P + b_1) + b_2],\qquad(5)$$

where P is input variable, T is output variable, f_1 is the activation function from input layer to hidden layer, f_2 is the activation function from hidden layer to output layer, w_1 is the weight matrix form input layer to hidden layer, w_2 is the weight matrix form hidden layer to output layer, b_1 is the threshold matrix from input layer to hidden layer, b_2 is the threshold matrix from hidden layer to output layer. The detailed values of the parameters are as follows:

$$w1 = \begin{bmatrix} 28.38 & -42.34 & -1.08 & 2.21 \\ 1.22 & 2.06 & -4.03 & 0.06 \\ 63.16 & 100.30 & -7.83 & 27.19 \\ 1.24 & 2.14 & -3.46 & 0.11 \\ 0.44 & 1.79 & -5.69 & -0.11 \\ -2.97 & -6.48 & 7.25 & -0.99 \\ 7.04 & 24.68 & 1.09 & -2.23 \\ 2.08 & -5.33 & 0.56 & -105.96 \\ 19.25 & 33.10 & -23.00 & 0.88 \\ -0.89 & -1.86 & 5.00 & 0.05 \\ 2.73 & 5.80 & -6.47 & 0.84 \end{bmatrix}, \quad b1 = \begin{bmatrix} -12.71 \\ 0.14 \\ -73.93 \\ 0.00 \\ 1.25 \\ -1.34 \\ -5.01 \\ 33.48 \\ -24.91 \\ -0.70 \\ 1.12 \end{bmatrix},$$

$$w2 = [169.95 \quad -85.10 \quad -0.07 \quad 46.94 \quad -27.58$$
$$-8.74 \quad 170.03 \quad -0.08 \quad 0.92 \quad -68.54 \quad -11.18],$$

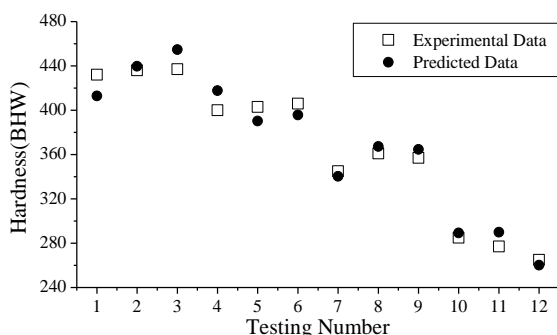$$b2 = [1.05], \quad f_1(x) = \frac{1 - e^{-2x}}{1 + e^{-2x}}, \quad f_2(x) = x.$$

FIGURE 7 Comparison of experimental data and predicted data for testing number after training

After network training, 12 experimental data used for network testing and get the predicted results. Then the outputs of the samples converted to the value of Brinell hardness by the way of reverse normalized. The testing results after transformation are shown in Fig. 7. The horizontal axle shows testing number, while the vertical axle illustrates the hardness of ADI of measured value and predicted value. In the previous diagram, the hollow squares and solid points represent the experimental data and prediction data, respectively. It can be obviously see that the predicted values approach to the measured data in most of the testing samples and indicated that the desired accuracy of the network model can be achieved. Therefore, the model based on artificial neural network can be applied in actual production with good accuracy. Table 2 are listed the absolute error of experimental and predicted value of the testing samples. It can be clearly see from the table that the maximum margin of error is 4.682%.

TABLE 2 Absolute errors of experimental data and predicted data for testing samples

	Experimental data (HBW)	Predicted data (HBW)	Absolute errors (%)
1	432	412.905	4.420
2	436	439.636	-0.834
3	437	454.745	-4.061
4	400	417.652	-4.413
5	403	390.215	3.173
6	406	395.656	2.548
7	345	340.374	1.341
8	361	367.252	-1.732
9	357	364.698	-2.156
10	285	289.265	-1.497
11	277	289.970	-4.682
12	265	260.247	1.794

5 Conclusions

From the study, the following conclusions can be drawn:

1. Increasing austempering temperature leads to a linear decreasing in hardness at the austempering times. The hardness of ADI slightly changed at different austempering time under the same temperature.

2. The detailed mathematical equation of the neural network model is available after the network training and the formula of the model is $T = f_2[w_2 f_1(w_1 P + b_1) + b_2]$. The detailed values of the parameters refer to the paper.

3. The predicted values approach to the measured data in most of the testing samples and indicated that the desired accuracy of the network model can be achieved. Therefore, the model based on artificial neural network can be applied in actual production with good accuracy.

4. The maximum margin of error between experimental and predicted data is 4.

75

References

[1] Han J M, Zou Q, Barber G C, Nasir T, Northwood D O, Sun X C, Seaton P 2012 Study of the effects of austempering temperature and time on scuffing behavior of austempered Ni–Mo–Cu ductile iron *Wear* **290-291** 99-105

[2] Eric O, Sidjanin L, Miskovic Z, Zec S, Jovanovic M T 2004 Microstructure and toughness of Cu Ni Mo austempered ductile iron *Materials Letters* **58** 2707-11

[3] Uma T R, Simha J B, Murthy K N 2011 Influence of nickel on mechanical and slurry erosive wear behaviour of permanent moulded toughened austempered ductile iron *Wear* **271** 1378-84

[4] Magalhaes L, Seabra J 1998 Wear and scuffing of austempered ductile iron gears *Wear* **215** 237-346

[5] Greno G L, Otegui J L, Boeri R E 1999 Mechanisms of fatigue crack growth in Austempered Ductile Iron *International Journal of Fatigue* **21** 35-43

[6] Sohi M H, Karshenas G, Boutorabi S M A 2004 Electron beam surface melting of as cast and austempered ductile irons *Journal of Materials Processing Technology* **153-154** 199-202

[7] Liu S F, Chen Y, Chen X, Miao H M 2012 Microstructures and mechanical properties of helical bevel gears made by Mn-Cu alloyed austempered ductile iron *Journal of Iron and Steel Research* **19**(2) 36-42

[8] Dias J F, Ribeiro G O, Carmo D J, Vilela J J 2012 The effect of reducing the austempering time on the fatigue properties of austempered ductile iron *Materials Science & Engineering A* **556** 408-13

[9] Liu S F 1999 The influence of heat treatment on the microstructures and properties of unalloyed austempered ductile iron *China Foundry Machinery & Technology* **3** 17-8

[10] Putatunda S K 2001 Development of austempered ductile cast iron (ADI) with simultaneous high yield strength and fracture toughness by a novel two-step austempering process *Materials Science and Engineering A* **315** 70-80

[11] Yang J H, Putatunda S K 2004 Improvement in strength and toughness of austempered ductile cast iron by a novel two-step austempering process *Materials and Design* **25** 19-230

[12] Li X F, Yu J, Liu L J, Liu H M, Zu F Q 2008 Effect of two-step austempering process on micrstructure and properties of austempered ductile iron *Transactions of Materials and Heat Treatment* **29**(2) 82-5

[13] Elsayed A H, Megahed M M, Sadek A A, Abouelela K M 2009 Fracture toughness characterization of austempered ductile iron produced using both conventional and two-step austempering processes *Materials and Design* **30** 1866-77

[14] Hsu C H, Lin K T 2011 A study on microstructure and toughness of copper alloyed and austempered ductile irons *Materials Science and Engineering A* **528** 5706-12

[15] Peng Y C, Jin H J, Liu J H, Li G L 2011 Effect of boron on the microstructure and mechanical properties of carbidic austempered ductile iron *Materials Science and Engineering A* **529** 321-5

[16] Yescas M A, Bhadeshia H K D H, MacKay D J 2001 Estimation of the amount of retained austenite in austempered ductile irons using neural networks *Materials Science and Engineering A* **311** 162-73

[17] PourAsiabi H, AmirZadeh Z, BabaZadeh M 2012 Development a multi-layer perceptron artificial neural network model to estimate the Vickers hardness of Mn-Ni-Cu-Mo austempered ductile iron *Materials and Design* **35** 782-9

[18] Ghaisari J, Jannesari H, Vatani M 2012 Artificial neural network predictors for mechanical properties of cold rolling products *Advances in Engineering Software* **45** 91-9

[19] Genel K 2004 Application of artificial neural network for predicting strain-life fatigue properties of steels on the basis of tensile tests *International Journal of Fatigue* **26** 1027-35

[20] Gencel O, Kocabas F, Gok M S, Koksal F 2011 Comparison of artificial neural networks and general linear model approaches for the analysis of abrasive wear of concrete *Construction and Building Materials* **25** 3486-94

[21] Calcaterra S, Campana G, Tomesani L 2000 Prediction of mechanical properties in spheroidal cast iron by neural networks *Journal of Materials Processing Technology* **104** 74-80

[22] Davim J P, Gaitonde V N, Karnik S R 2008 Investigations into the effect of cutting conditions on surface roughness in turning of free machining steel by ANN models *Journal of Materials Processing Technology* **205** 16-23

[23] Salman S, Fındık F, Topuz P 2007 Effects of various austempering temperatures on fatigue properties in ductile iron *Materials and Design* **28** 2210-4

[24] Kowalski A, Tybulczuk J 2002 Influence of heat treatment parameters on the structure and property of Ni-Cu alloyed ADI *Foundry* **151**(11) 698-700

[25] Peng Y C, Jin H J, Liu J H, Li G L 2012 Influence of cooling rate on the microstructure and properties of a new wear resistant carbidic austempered ductile iron (CADI) *Materials Characterization* **72** 53-8

[26] Lin C K, Lai P K, Shih T S 1996 Influence of microstructure on the fatigue properties of austempered ductile irons - High-cycle fatigue *International Journal of Fatigue* **18**(5) 297-307

[27] Wei D Q 2005 Effect of alloying elements on structure and mechanical properties of bainite ductile Iron in the step austempering in machine oil at room temperature *Materials for Mechanical Engineering* **29**(12) 29-32

[28] Sohi M H, Ahmadabadi M N, Vahdat A B 2004 The role of austempering parameters on the structure and mechanical properties of heavy section ADI *Journal of Materials Processing Technology* **153-154** 203-8

[29] Wang W, Guo X H, Wang C H, Wang H 2010 Research on the influence of heat treatment parameter on the mechanical property of austempered ductile iron *International Conference on Mechanic Automation and Control Engineering, 26-28 June 2010* 5918-21

[30] Liu G J, Wang T X 2001 Effect of isothermal quenching temperature on mechanical properties of austempered ductile iron *Foundry* **50**(9) 567-9

[31] Podgornik B, Vizintin J, Thorbjornsson I, Johannesson B, Thorgrimsson J T, Celis M M, Valle N 2012 Improvement of ductile iron wear resistance through local surface reinforcement *Wear* **274-275** 267-73

[32] Kim Y J, Shin H, Park H, Lim J D 2008 Investigation into mechanical properties of austempered ductile cast iron (ADI) in accordance with austempering temperature *Materials Letters* **62** 357-60

[33] Zhu J W 2002 The influences of austempering process on the mechanical properties of nodular graphite cast iron *Journal of Jilin Institute of chemical Technology* **19**(1) 51-3

Authors

Guo Xuhong, born on June 22, 1963, Gansu, China

Current position, grades: professor in Soochow University
University studies: Department of Mechanical Engineering in Lanzhou university of technology
Scientific interest: Cutting mechanism, precision finishing, Process parameters optimization.
Publications: 2 Patents, 40 Papers
Experience: 1998 - present, working in school of mechanical and electric engineering, Soochow University. 1997 - 1998, further studying in Sunny electronic (Nagano, Japan) Co. 1996 - 1997, teaching in Department of Mechanical Engineering of Soochow silk engineering college. 1990 - 1995, teaching in process department of Hubei University of Automotive technology. 1987- 1990, Studying for a master's degree in Metal processing laboratory of South China University of Technology. 1983-1987, working in Hubei University of Automotive technology. 1979 - 1983, studying for a bachelor's degree, majoring in manufacturing technology and equipment in Lanzhou university of technology.